RADIATION PATTERN CHANGES OF A NORMAL-MODE HELICAL ANTENNA INSIDE HUMAN BODY FOR USE IN HUMAN BODY SENSING

Rasyidah Hanan Binti Mohd Baharin, Nguyen Thanh Tuan, Yoshihide Yamada†
†Malaysia-Japan International Institute of Technology, Universiti Teknologi Malaysia, Kuala Lumpur, Malaysia
†rh.baharin@gmail.com

Kamilia Binti Kamardin††
††Advanced Informatics School, Universiti Teknologi Malaysia, Kuala Lumpur, Malaysia
††kamilia@utm.my

ABSTRACT

In recent years, many types of radio sensors are being developed for health monitoring system. RF device for human body such as Wireless Capsule Endoscopy (WCE) requires the antenna to be miniaturized. Normal-Mode Helical Antenna (NMHA) is a promising candidate due to its high efficiency in small size. To understand the situation of antenna inside a dielectric material, a study using electromagnetic simulation was made. In this paper, a simulation model of NMHA inside human body is presented. Practically, shifting of antenna inside human body may happen. Changes of input impedance and radiation pattern are observed at Medical Implant Communications Service (MICS) frequency of 402MHz. The obtained results help to understand the possibility of NMHA implementation in human body sensing.

1. INTRODUCTION

Biomedical telemetry devices are a set of system that allows physical signal to be measured at a distance. The physical signal is then obtained by using suitable circuit, post-processed, and eventually transmitted externally for health monitoring. It is generally divided into ingestible, implantable and wearable device [1]. WCE is an ingestible type and the antenna is an important component for transmission and reception of signal. The physical characteristic of the antenna will determine the quality of images received in real-time.

Previously developed antenna for WCE includes outer-wall loop antenna [2], spiral antenna [3], and plannar slotted patch antenna [4]. However, due to the miniaturization requirement, the antenna efficiency is sometimes compensated for it to be small in size. NMHA is a potential candidate that has small size and high efficiency. Because of the small coil structure of the NMHA, antenna size is effectively reduced. Moreover, the coil structure produces two radiation sources such as electric and magnetic currents. Hence, high antenna efficiency is expected. Another benefit of a coil structure is achieving self-resonant characteristics [5][6].

In the case of applying NMHA to a human body, the human body condition of a lossy material with high permittivity and conductivity should be taken into account and the electrical characteristics in such condition should be studied [7].

In this paper, NMHA performance inside stomach tissue is studied using computational electromagnetic simulator FEKO 7.0 by Method of Moment (MoM). A model of NMHA embedded inside dielectric material with similar electrical characteristic of real stomach. The simulation model is then repeated to the case of antenna shift inside the stomach path. The resonant structure, input impedance and radiation pattern is observed. Based on the data obtained from simulation, the fundamental of NMHA for application in ingestible WCE can be understood more.

2. ANTENNA FOR ENDOSCOPIC CAPSULE

Fig. 1 (a) shows Endocapsule 10, one of the commercialized WCE that is currently available. Meanwhile, Fig. 1(b) is a cross section of proposed magnetic-propelled endoscopic system by Gao et. al., whereby one of the major component is antenna.

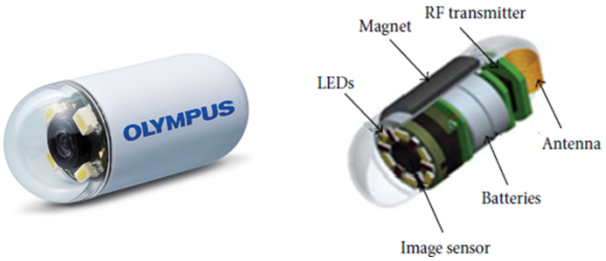

(a) Endocapsule 10 (b) Cross section WCE

Fig. 1 Endocapsule 10 by Olympus Corp. [8], and (b) Cross section of WCE design by Gao et. al. [9]

Generally, all WCE are equipped with a compact body with sensing elements and image capture system.

The sensing element consists of a very small antenna that acts as a transmitter and receiver of data from human body. Since NMHA is an omni-directional antenna, it is suitable for the random orientation for sensors inside human body.

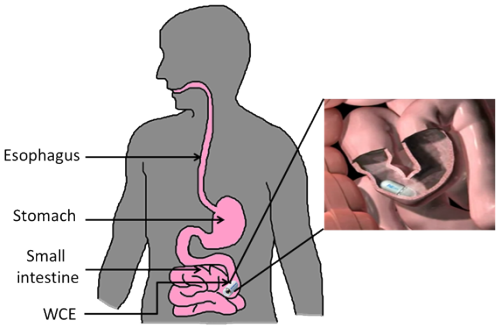

Fig. 2 WCE in human body

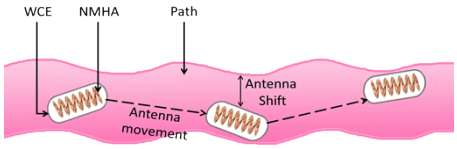

Fig.3 Antenna shift when traverse

Fig. 2 show how the WCE traverse along the small intestine. Fig. 3 visualize the movement could possibly cause the antenna to shift along the selected human tissue and change its electrical characteristics.

3. SIMULATION PARAMETERS

3.1. Simulation model

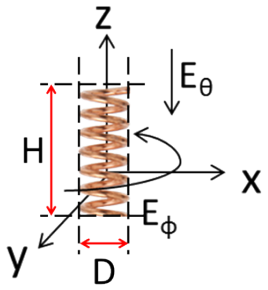

Fig. 4 NMHA structure

NMHA structure is shown in Fig. 4 [10]. The radiation is divided into E_ϕ and E_θ component. By adjusting the height (H) and diameter (D) of the antenna, we can obtain the resonance structure where the input impedance (Z_{in}) becomes pure resistance (R_{in}) at the operated frequency.

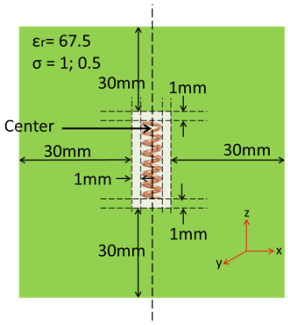

Fig. 5 Simulation model NMHA inside stomach

A simplified simulation model of NMHA inside human phantom was made to study the situation of antenna shift. Fig. 5 shows the original setup in which the antenna is placed at the center of the phantom. The simulation was also repeated for σ=0.5 to study the effect of lower conductivity. Simulation parameters used are summarized in Table 1.

Table 1 Simulation parameters of NMHA in stomach

Software	FEKO 7.0 (MoM)
Frequency	MICS standard at 402MHz
Antenna	H/λ_g= 0.2; D/λ_g=0.115 10.4mm x 18.15mm (D x H)
No. of turns	N= 7
Metallic wire	Copper (σ = 58 x 10^6 [1/Ωm]), Diameter, d = 0.5mm
Dielectric constant of stomach tissue [11]	ε_r= 67.5 ; μ_r=1; σ=1, σ=0.5 Mass density = 1050kg/m^3 Shift distance, *b*=5;10; 15(mm)
Mesh size	Phantom = $\lambda_g/20$ Antenna = $\lambda_g/100$
Memory	500 MB
Calculation time	0.13 hour /sim

3.2. Self-resonant structure of NMHA inside stomach tissue

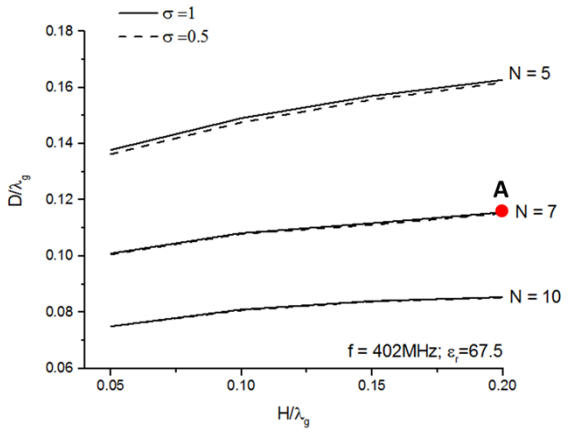

Fig. 6 Self-resonance curve of NMHA

Fig. 6 shows the self-resonance characteristics of NMHA for conductivity σ=1 and σ=0.5 inside the stomach tissue, with permittivity ε_r=67.5 at 402MHz. It can be seen that for different conductivity, it does not affect the resonant structure greatly. For the purpose of this simulation, we have chosen point A where the dimension of antenna is given by 10.41mm x 18.15mm (D x H).

4. SIMULATION RESULTS

4.1. Antenna shift simulation model

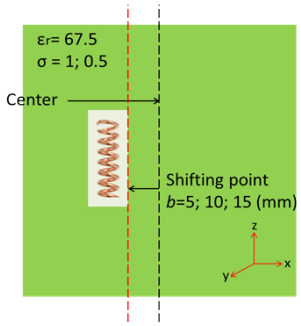

Fig. 7 Simulation model NMHA shifted

Fig. 7 models the antenna when shifted from the center by a distance (noted by parameter *b*), *b*=5; 10; 15 as it traverse along the stomach path. The results and comparison with the original model is calculated from the simulation will be discussed in the next section.

4.2. Input Impedance

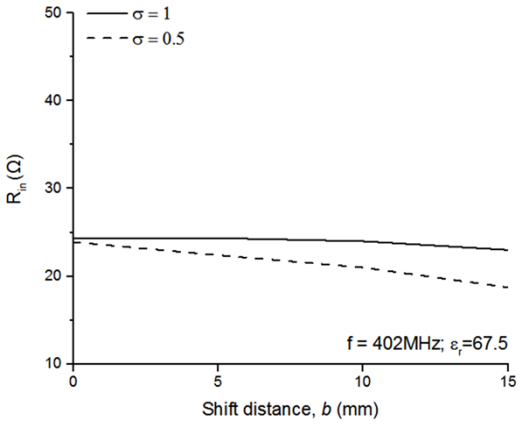

Fig. 8 Input impedance

The input impedance is shown in Fig. 8. The input impedance R_{in} not changed greatly with the shifting of antenna. For the case of σ=0.5 the input impedance obtained by antenna is lower than when phantom conductivity, σ=1. The input impedance becomes lower because the wave is travelling in a less lossy medium.

4.3. Radiation Pattern

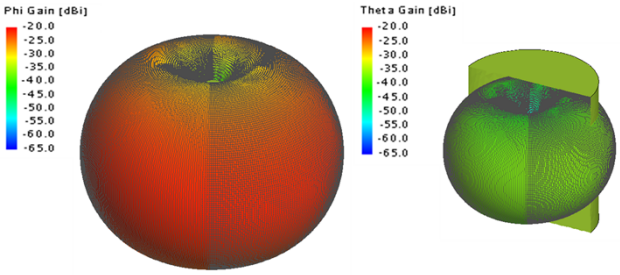

(a) E_ϕ (b) E_θ

Fig. 9 3D Radiation pattern

The 3D radiation characteristic for the original setup, with antenna at the center, (σ=1; *b*=0) is shown in Fig. 9. For NMHA inside stomach phantom, the E_ϕ component is larger than the E_θ component, thus the maximum radiation is from E_ϕ. The directivity is calculated at E_ϕ as -21.7dBi.

However, since the antenna is shifted only along the x-axis of the antenna and phantom, the polar radiation pattern is observed from the horizontal cut (xy-plane) next.

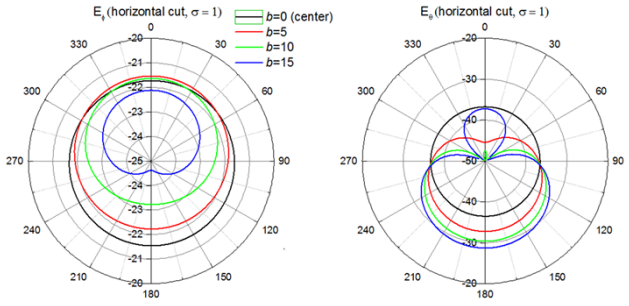

(a) E_ϕ (b) E_θ

Fig. 10 Radiation pattern for σ=1 (xy-plane)

Fig. 10 shows the polar plot at horizontal cut for phantom conductivity, σ=1. When antenna is not shifted (*b*=0), $E_{\phi max}$ and $E_{\theta max}$ is calculated to be -21.7dBi and -36.7dBi respectively. From the shifting it is observed that the changes in E_ϕ is small, however it is distortion occurs at larger value of *b*. Meanwhile at E_θ, the distortion are more apparent, however still gain level are still smaller compared to E_ϕ.

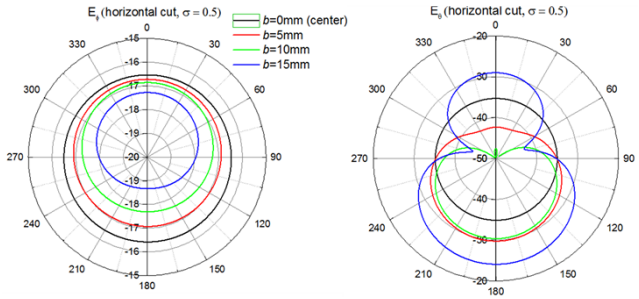

(a) E_ϕ (b) E_θ

Fig. 11 Radiation pattern for σ=0.5 (xy-plane)

To study the effect of different conductivity, the radiation pattern was observed for σ=0.5. Fig. 11 (a) and Fig. 11 (b) shows the polar plot at horizontal cut for σ=0.5. At the center (*b*=0), $E_{\phi max}$ and $E_{\theta max}$ is calculated to be -16.5dBi and -34.9dBi respectively. At lower conductivity, the gain level is expected to be higher because resistance of material is lower.

Compared with material σ=1, the characteristic of radiation is observed to be similar, in which maximum radiation is from E_ϕ. Distortion is clearly more on E_θ component. As the value of *b* is larger, E_θ loses more of its omni-directional characteristics and the radiation become more dominant. For on the application of WCE, the major change in radiation pattern may pose a problem for signal reception or transmission.

5. CONCLUSION

A possible case of antenna shifting effect inside the stomach is modeled. For σ=1, the resonance structure and input impedance is not affected by the shifting. At larger shifting value, radiation pattern on horizontal cut E_ϕ becoming more suppressed and E_θ loses its omni-directional characteristic. The simulation was also repeated with lower conductivity σ=0.5. In this condition, the input impedance becomes lower and the gain level is higher. Change in radiation pattern is more apparent that of σ=1. By clarifying simulation results, it helps to understand the possibility of NMHA for application in human body sensors.

6. REFERENCES

[1] Konstantina S. Nikita, IEEE Press Series in Biomedical Engineering, in Handbook of Biomedical Telemetry, Wiley-IEEE Press, New Jersey, 2014.

[2] S. Yun, K. Kim, S. Nam, "Outer-Wall Loop Antenna for Ultrawideband Capsule Endoscope System," IEEE Antennas and Wireless Propagation Letters, vol. 9, pp. 1135-1138 (2010).

[3] A.P. George, M. Sujatha, G.L.G. Anandhi: "Design and Simulation of Spiral Antenna for Endoscope," International Journal of Engineering Research & Technology, Vol.2, Issue 11 (2013).

[4] F. Arifin, P. K. Saha, "Design of a miniaturized UWB ingestible antenna for Wireless Capsule Endoscopy," International Conference on Advances in Electrical Engineering (ICAEE), pp. 51-54, (2015).

[5] Y.Yamada, N.Michishita,"Design Methods and Electrical Performances of Small Normal-Mode Helocal Antennas," IEICE Trans. Commun. B, Vol. J96-B, No. 9, pp. 894-906 (2013).

[6] Q.D. Nguyen, N. Michishita, Y. Yamada, K. Nakatani, "Determnistic Equation for Self-Resonant Structures of Very Small Normal-Mode Helical Antennas," IEICE Trans. Commun., vol.E94-B, No.5, pp.1276-1279 (2011).

[7] N. T. Tuan, Y. Yamada, N. Q. Dinh and N. Michishita, "Self-resonant structures of normal-mode helical antennas embedded in dielectric and magnetic materials," International Conference on Advanced Technologies for Communications (ATC), pp. 627-632 (2015).

[8] Endocapsule 10, https://www.olympus-europa.com/medical/en/medical_systems/products_services/product_details/product_details_74304.jsp (2016).

[9] M. Gao, C. Hu, Z. Chen, H. Zhang, S. Liu, "Design and Fabrication of a Magnetic Propulsion System for Self-Propelled Capsule Endoscope," IEEE Transactions on Biomedical Engineering, Vol. 57, No. 12, pp. 2891-2902 (2010).

[10] J. D. Kraus, "The Helical Antenna," Proc. IRE, Vol. 37, No. 3, pp. 263–272 (1949).

[11] J. Kim and Y. Rahmat-Samii, "Implanted antennas inside a human body: simulations, designs, and characterizations," IEEE Transactions on Microwave Theory and Techniques, Vol. 52, No. 8, pp. 1934-1943(2004).